Turkish J. Eng. Env. Sci.
28 (2004) , 249 – 259.

Fracture Assessment of Welded Steel Structures Using the SINTAP

Binnur GÖREN KIRAL, Seçil ERİM
Dokuz Eylül University, Department of Mechanical Engineering, İzmir-TURKEY
e-mail: binnur.goren@deu.edu.tr

Received 01.03.2004

Abstract

The assessment of weld defects is entirely related to the reliability of the beam-to-column connections in welded steel structures. This paper aims to determine accurate and quick defect assessment of welded steel structures and to compare the fracture behavior of different connection types using the Structural Integrity Assessment Procedure (SINTAP). The SINTAP-Level II for welded structures and the net-section-collapse method to determine the limit loads of each connection having various sizes of semi-elliptical crack configurations are used for the development of structures prone to earthquakes. Weld defects modeled as surface cracks are taken through the heat-affected zone at connections where the column flange meets the bottom flange of the beam. The procedure described in this study allows the assessment of the maximum crack size permitted in the welded connection under loading without the occurrence of a brittle fracture. The results obtained from the present study agree well with those of the other studies. This procedure also reduces the time of analysis and enables one to examine the effects of variables such as the material properties of the base or weld metal, connection type and the crack size on the fracture behavior of the structure.

Key words: SINTAP, Net-section-collapse method, Welded column-beam connection, Brittle fracture.

Introduction

The Marmara earthquake on August 17, 1999, of 7.4 magnitude caused a devastating catastrophe and thousands of people died in the collapse of numerous concrete buildings, the predominant structural system used for buildings in Turkey. This system consists of reinforced concrete frames with unreinforced masonry infills. This structural form is used for all building heights and occupancy, from single-storey commercial to multi-storey residential and office buildings. Industrial buildings are either reinforced concrete (cast-in-place or pre-cast) or steel frame structures.

An alternative to concrete, steel, by far the most expensive construction material in Turkey, has been used rather sporadically in construction; only industrial structures rely on steel for their lateral load resistance. Some steel structures were damaged by this earthquake and only a few collapsed. The main collapse was generally at the column-to-beam connection in the form of tearing of the weld connecting columns-to-beams, fractures of brace connections, and buckling of braces. Other collapses included failure of anchor bolts at column bases and structural instability under overturning forces. Further evidence of damage includes local buckling in concrete filled steel hollow pipes used as wharves.

However, it is not sufficient to use steel structures in seismic areas in order to avoid earthquake damage. The Kobe (Japan, January 17, 1995) and Northridge (US, January 17, 1994) earthquakes caused serious damage to some welded steel structures by unexpected failure in a brittle manner. The 1994 Northridge and 1995 Kobe earthquakes resulted in unexpected and serious damage in a very large number of welded steel moment resisting connections, which were specially designed to respond in a ductile manner to have appropriate energy absorption by plastic deformation under seismic conditions. The

post-earthquake investigations revealed that the design and material properties of the connections were the causes of the brittle fractures. Many fractures occurred in the weld root at the bottom flanges of the beams (Toyoda, 2002).

Azuma *et al.* (2000) investigated beam-to-column connections with weld defects by testing them under cyclic loads and evaluated the fracture toughness properties of numerically modeled weld defects.

Kuntiyawichai and Burdekin (2003) studied the effects of dynamic loading on both fracture toughness specimens under rapid loads and cracked connections in steel framed structures under earthquake loads using the finite element method.

Righiniotis *et al.* (2000) simplified a 2-dimensional crack model for assessing the fracture of bottom flange welds in steel beam-to-column connections and presented the formulation of the approximate expressions for the stress intensity factors related to the cracked geometry accounting for typical stress conditions.

However, there remain some problems to be solved for clarifying the engineering fracture assessment method. In the present study, 4 types of welded steel beam-to-column connections having different dimensions including crack-like defects are examined using the Structural Integrity Assessment Procedure (SINTAP) Level II European flaw assessment procedure for mismatched stuctures. The limit loads for each connection are determined by the net-section-collapse (NSC) method.

The aim of this study was to assess the safety of welded steel beam-to-column connections under loadings as in earthquake loads in order to avoid brittle fractures. The limit and maximum loads, and the critical crack length of each connection were determined and compared for each connection type under various loading conditions. Finally, improvement of the welded steel structure to withstand the earthquake was aimed using analytical methods.

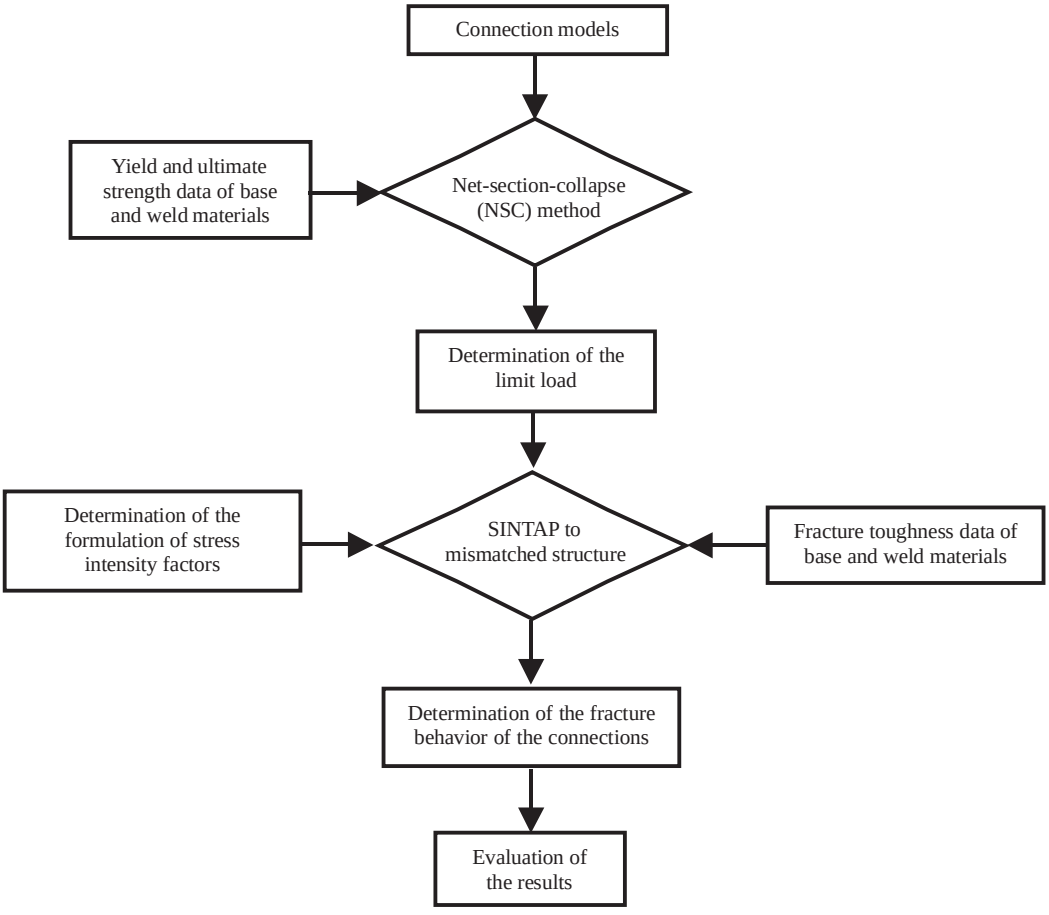

Figure 1. Flow scheme.

Analysis procedures

The NSC method and SINTAP were applied to welded steel structures in order to determine their fracture behavior under instantaneous intense load as in earthquakes. Determining the connection models was the first step of the analysis. The NSC method was used for obtaining the limit load values of the connections. The yield and ultimate strength values of base and weld materials should be known for the NSC method. SINTAP requires the formulation of the stress intensity factor of each connection, fracture toughness values of base and weld material and the limit load. SINTAP gives the fracture behavior of a connection under loading. The analysis stages followed in this study are given in Figure 1 as a flow scheme.

Beam-to-column connection and crack models

The welded steel structure subjected to earthquake loads is given in Figure 2. The connections investigated consist of W30 × 99 beams connected to W14 × 176 columns by welding. The materials of the beam and column are both A 572 steel Gr. 50 and the flange welds are made with an E70TG-K2 electrode.

The welded steel structure is subjected to vertical force at the end of the beam. This force, which causes the bending moment, simulates earthquake loads. Although cracks may be exposed to shear, experience shows that only the tensile stress normal to the crack is important in causing fatigue or fractures in steel structures (BSI, 1991). Therefore, this loading case was considered.

A semi-elliptical surface crack was placed through the heat-affected zone at the connection where the column flange meets the bottom flange of the beam. The dimensions of the semi-elliptical surface crack are given in Figure 3, where a denotes crack length and crack width is (AWS, 2000)

$$c = 1.5a \tag{1}$$

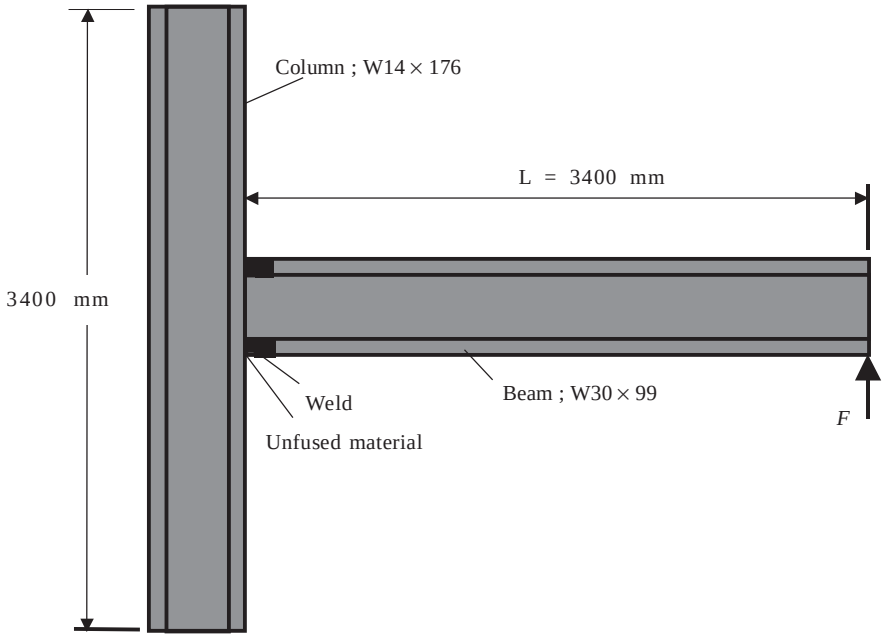

Figure 2. Beam-to-column configuration.

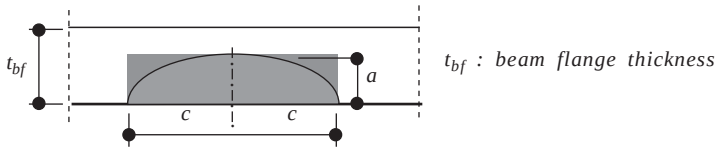

Figure 3. Dimensions of the semi-elliptical surface crack.

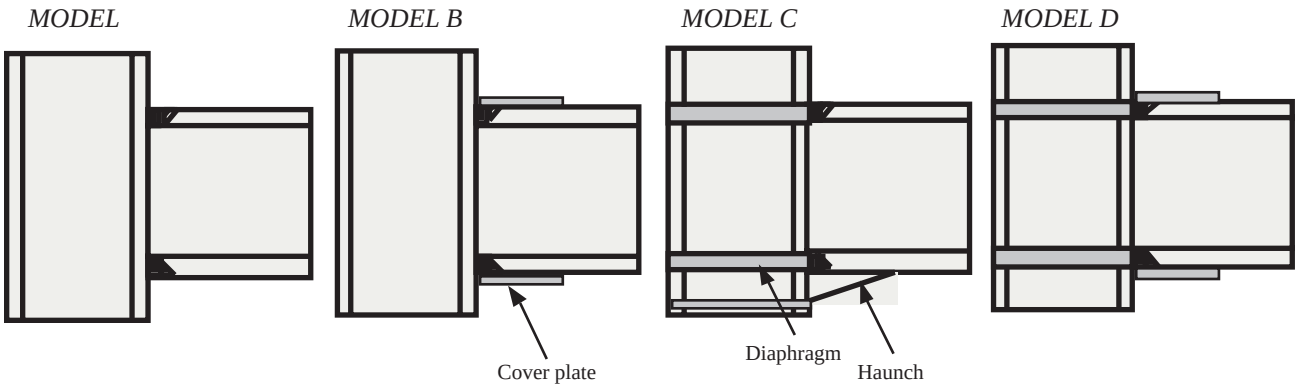

Figure 4. Beam-to-column connection details.

In order to determine the effect of the connection design on the fracture behavior, models consisting of beam-to-column connections of 4 different types were chosen (Figure 4).

Model A is the basic connection used before the Northridge earthquake. Model B has cover plates whose thicknesses are taken as 10 mm, 20 mm and 25 mm in order to further estimate the effects of thickness. Models C and D have connections with an additional haunch-diaphragm and cover plate-diaphragm, respectively. The cover plate thicknesses in Model D are 10 mm and 20 mm.

The semi-elliptical surface crack is placed in the heat-affected zone beneath the beam bottom flange in each model.

Material properties

As can be seen in Table 1, electrode E70T-4 is a low toughness flux core electrode and it was commonly used in steel structures before the 1994 Northridge earthquake. In this study, electrode E70TG-K2, which is more ductile than electrode E70T-4, is used for the welded joint.

K_{mat}, fracture toughness, is calculated using the fracture toughness value obtained by Charpy V-Notch (CVN) testing. Due to expense and size limitations associated with fracture toughness tests, it is useful to make estimations of fracture toughness from CVN toughness requirements. The empirical correlation between CVN and K_{mat} is as follows (Koçak and Motarjemi, 2002):

$$K_{mat} = \sqrt{\frac{E\,(0.53CVN^{1.28}) \times 0.2^{(0.133CVN^{0.256})}}{1000\ \ (1-\upsilon^2)}} \tag{2}$$

where K_{mat} in MPa$\sqrt{m}$ and CVN in joules.

Limit load estimation

The limit load, which is the main input for SINTAP, is determined using the NSC method for each beam-to-column connection under loading. This method is based on the static equilibrium of forces and moments (Rahman, 1998; Kim *et al.*, 2003).

The structure is subjected to bending moment that simulates earthquake loading as shown in Figure 5. The location of the plastic neutral axis is obtained from the equilibrium of horizontal forces along the z-axis (Kim *et al.*, 2003).

Table 1. Material properties of base and weld material at 21 °C (Chi, 1999).

	Yield Strength (MPa)	Ultimate Strength (MPa)	Elasticity Modulus (GPa)	Fracture Toughness (MPa$\sqrt{m}$)
Weld (E70T-4)	420	725	210	85
Weld (E70TG-K2)	485.8	605.6	201.2	120
Base Metal (A 572)	347	433.7	204.1	250

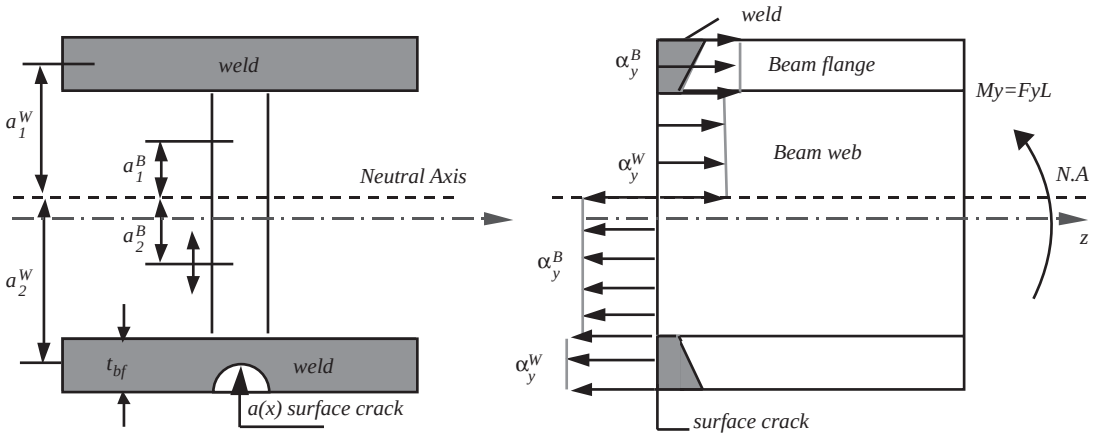

Figure 5. Resulting stress distribution under loading.

The limit load can be determined as follows:

$$F_Y + \sum \left(\sigma_y^W A^W + \sigma_y^B A^B\right) = 0 \tag{3}$$

$$M_Y + \sum \left(\sigma_y^W A^W a^W + \sigma_y^B A^B a^B\right) = 0 \tag{4}$$

where F_y and M_y are the limit load and limit moment of the connection, respectively. σ_y^B and σ_y^W are the yield strength of the base and weld material, namely A 572 Gr. 50 steel and E70 TG-K2, respectively (Table 1). a^W and a^B are the distances from the centroid of the flanges and the web to the neutral axis.

Stress intensity factor formulations

For Mode I, which corresponds to in-plane tensile crack opening, the stress intensity factor for arbitrary loading is expressed in the general form as (Murakami, 1987)

$$K_I = \sigma\sqrt{\pi a} Y\left(a/t_{bf}\right) \tag{5}$$

where σ is the characteristic remotely applied stress

$$\sigma = \frac{My}{I} = \frac{F \cdot 3400 \cdot y}{I} \tag{6}$$

y is the distance from the x-axis to the point where the stress is calculated, L is the length of the beam and I is the moment of inertia for the area with the semi-elliptical crack. F is the applied load related to the limit load and it is given as

$$F = L_r F_Y \tag{7}$$

$Y(a/t_{bf})$ is the Mode I stress magnification factor, which depends on the type of loading. Stress magnification factors are related to specific a/t_{bf} ratios for the geometry under bending (Figure 6). Polynomial expressions for the bending are given by

$$\begin{aligned} Y\left(a/t_{bf}\right) = {} & 944.85\left(\tfrac{a}{t_{bf}}\right)^6 - 2290.5\left(\tfrac{a}{t_{bf}}\right)^5 \\ & +2168.2\left(\tfrac{a}{t_{bf}}\right)^4 - 1003.2\left(\tfrac{a}{t_{bf}}\right)^3 \\ & +237.75\left(\tfrac{a}{t_{bf}}\right)^2 - 27.098\left(\tfrac{a}{t_{bf}}\right) + 2.1681 \end{aligned} \tag{8}$$

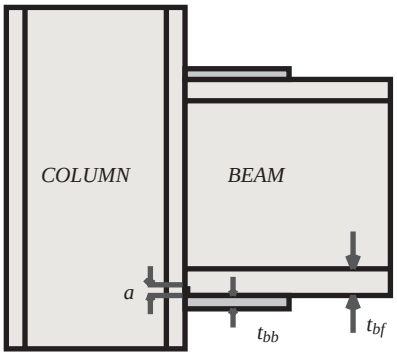

Figure 6. The beam-to-column connection with the surface crack.

K_I can be expressed for a semi-elliptical weld defect under bending (Righiniotis *et al.*, 2002):

$$K_I = \sigma\sqrt{\frac{\pi a}{Q}} Y \frac{Y_1}{Y_2} \tag{9}$$

Y_1 and Y_2 are given by

$$Y_1 = 1.0807 \left(\frac{\frac{a}{t_{bf}}}{\frac{a}{t_{bf}} + \frac{t_{bb}}{t_{bf}}} \right)^{-0.3299} \qquad Y_2 = 1.12 \quad (10)$$

Q is the elliptical shape correction factor given by

$$Q\,(a/c) = 1 + 1.464 \left(\frac{a}{c} \right)^{1.65} \qquad (11)$$

Application of SINTAP

SINTAP is used to evaluate structural integrity in European industry and its main output is flaw assessment (Ainsworth *et al.*, 2002). It was developed by the GKSS Research Center in Germany for mismatched welded structures. The SINTAP mismatch procedure provides confidence in the assessment of defective weld strength mismatched structures (Kim *et al.*, 2000; Kim and Schwalbe, 2001; Koçak and Motarjemi, 2002).

Basic equations

SINTAP includes crack driving force (CDF) and failure assessment diagram (FAD) routes. In the CDF route, the material resistance against the crack growth (R-curve) is compared with the crack tip loading in the component (Figure 7). In the FAD route, a failure line is constructed by normalizing the crack tip loading (or applied stress intensity factor) with respect to the material's fracture toughness. In this paper, the FAD approach and Level II, which requires yield and ultimate strengths, are used.

In the FAD approach, the basic equation is

$$K_r = f(L_r) \qquad (12)$$

L_r is the ratio of the applied load, F, to the plastic yield load of the mismatched structure, F_Y. F_Y is calculated by the NSC method:

$$L_r = \frac{F}{F_Y} \qquad (13)$$

Confidence in the structure requires that

$$K_r = \frac{K_I}{K_{mat}} \leq f(L_r) \qquad (14)$$

where K_I is the stress intensity factor of the structure, and K_{mat} is the fracture toughness of the material in which the crack is placed (in this study the fracture toughness of the weld metal).

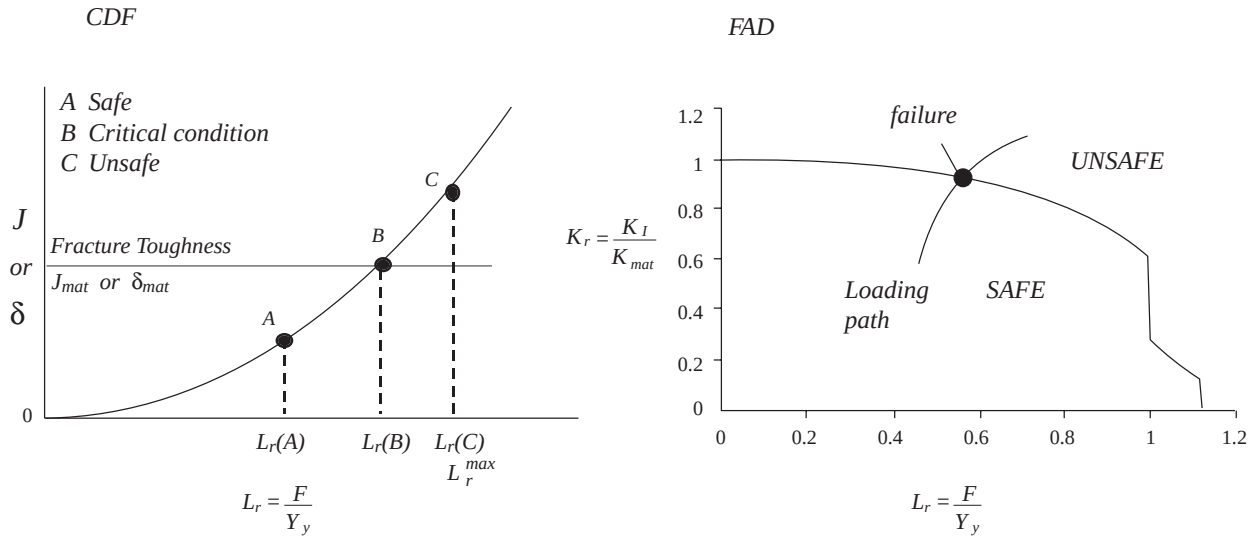

Figure 7. Presentation of CDF and FAD.

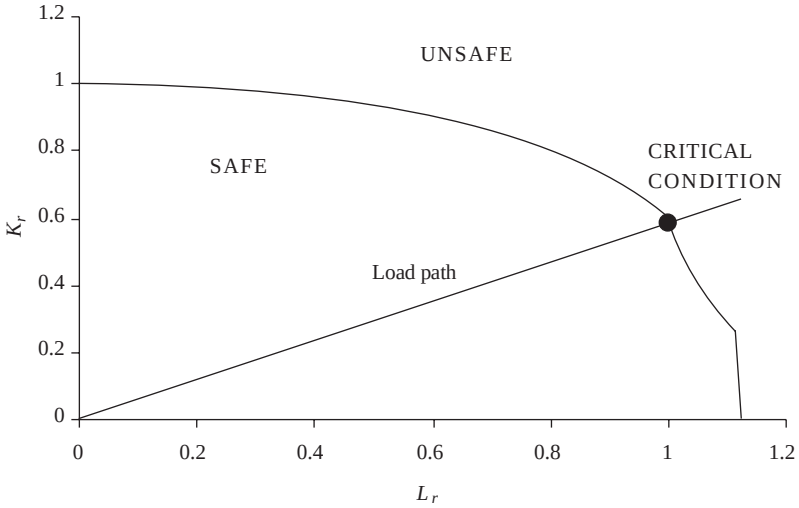

Figure 8. SINTAP Level II (mismatch)-FAD route for Model A.

Results

In this study, the critical crack size, a_{cr} that the structure can withstand under numerous loading conditions is presented. a_{cr} occurs for the case where the load path intersects the FAD curve and it is obtained by Eqs. (9), (12) and (14). These equations are related to both the crack length and the applied load. That is, a_{cr} is determined by considering the change in both the crack length and the load. Figure 8 shows the SINTAP-FAD diagram, which is used in the analysis Level II, for Model A. Computer codes are developed using MATLAB 6.1 software for the calculations. These computer codes are capable of considering the effects of numerous parameters such as connection type, material properties and crack size.

The approximate limit load values for each connection containing semi-elliptical surface cracks are presented in Table 2 under the effect of bending moment. The limit load values that are calculated by Eq. (3) are for welded mismatched structures.

As seen from the table, for Models A and B these values are well below those of other connection types. Model C is the most resistant connection when considering the limit load values of all models. Use of the bottom haunch and diaphragm increases the limit load of the welded steel connection. Kuntiyawichai and Burdekin (2003) also emphasized the affirmative effect of the bottom haunch and cover plates on the fracture.

Figures 9a and b illustrate the performance of the strengthened connection types in comparison with Model A, which is the weakest connection type. These figures show the effect of using cover plates, diaphragms and an additional haunch in the steel welded structures on their limit and maximum loads. Maximum performance was obtained using Model C, as seen from the figures. There was a significant increase in the limit load of about 137% compared with Model A. The limit load increased about 75% when Model D was used. The results also show that there were no extreme changes with a 100% increase in thickness of the cover plate considering Models B and D. These values were about 3.1% and 1.7% for Models B and D, respectively.

Table 2. Approximate limit load values for welded beam-to-column connections.

Connection Types	Limit Load Values (N)
A	379,067
B1 (t_{bb} = 10 mm)	379,185
B2 (t_{bb} = 20 mm)	379,303
B3 (t_{bb} = 25 mm)	379,363
C	898,688
D1 (t_{bb} = 10 mm)	662,486
D2 (t_{bb} = 20 mm)	662,604

Figure 9b shows the effect of connection type on maximum load. There are tendencies in the maximum load variation similar to those in the limit load,

as shown in Figure 9a. Maximum performance was obtained using Model C as the welded joint in the steel structure compared with Model A. The maximum load value of this connection type was about 137% higher. This increase was about 75% when Model D was used.

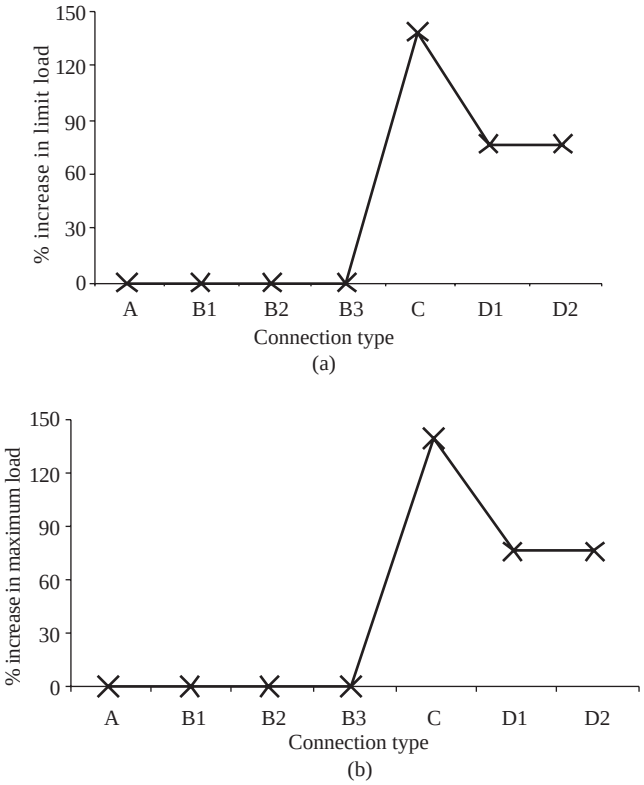

Figure 9. Comparison of (a) limit and (b) maximum loads of the connection types.

Figure 10 shows the variation of the critical crack length versus the load applied. Each graph presents the maximum critical crack length that the connection can stand unless a brittle fracture occurs under loading. The curves assess the load-carrying capacities of the beam-to-column connections with the surface elliptical cracks. If the applied load for any crack length remains under the curve, the system is considered safe. Otherwise, a brittle fracture may occur unexpectedly.

When the results of Models A and B are examined, there seems to be no substantial difference regarding the limit and maximum load values and the critical crack length.

As shown in Figures 10e and 10g, there are 2 extreme critical crack lengths. The critical crack length decreases as the applied load reaches the limit load. When the ligament collapse occurs, a crack length larger than that in the elastic region close to the limit load can be permitted. Although the same tendency can be seen when the Model A is used, this region is more limited in comparison with that of strengthened connections.

The results agree well with those of other studies. Fisher *et al.* (1998) showed that a structure having a 19 mm crack length fails at a remote tensile stress value of 160 MPa for electrode E70T-4, and 178 kN vertical force caused this stress value in the welded steel structure, which has the connection type Model A. In this study, critical crack size was 19.67 mm under this loading condition for electrode E70T-4.

Table 3 presents the permissible crack size for each model when the structure is subjected to a load of 100 kN magnitude.

Table 3. Comparison of the critical crack length size of structures subjected to loads at relatively low levels (F= 100 kN).

Connection types	Critical crack length size (mm)
A	22.10
B1	22.05
B2	22.55
B3	22.78
C	20.63
D1	22.06
D2	22.55

Although it is expected that larger critical crack sizes can be permitted in strengthened connections, Table 3 and Figure 10 show that the critical crack lengths of all connections become rather close to each other when beam-to-column connections are subjected to loads at relatively low levels. This situation arises because of the stress concentration due to the geometrical discontinuities in the strengthened connections. Nevertheless, especially when the structure is liable to instantaneous intense loads, use of such connections will be safe. It is obvious that these connections are suitable for steel structures in seismic areas.

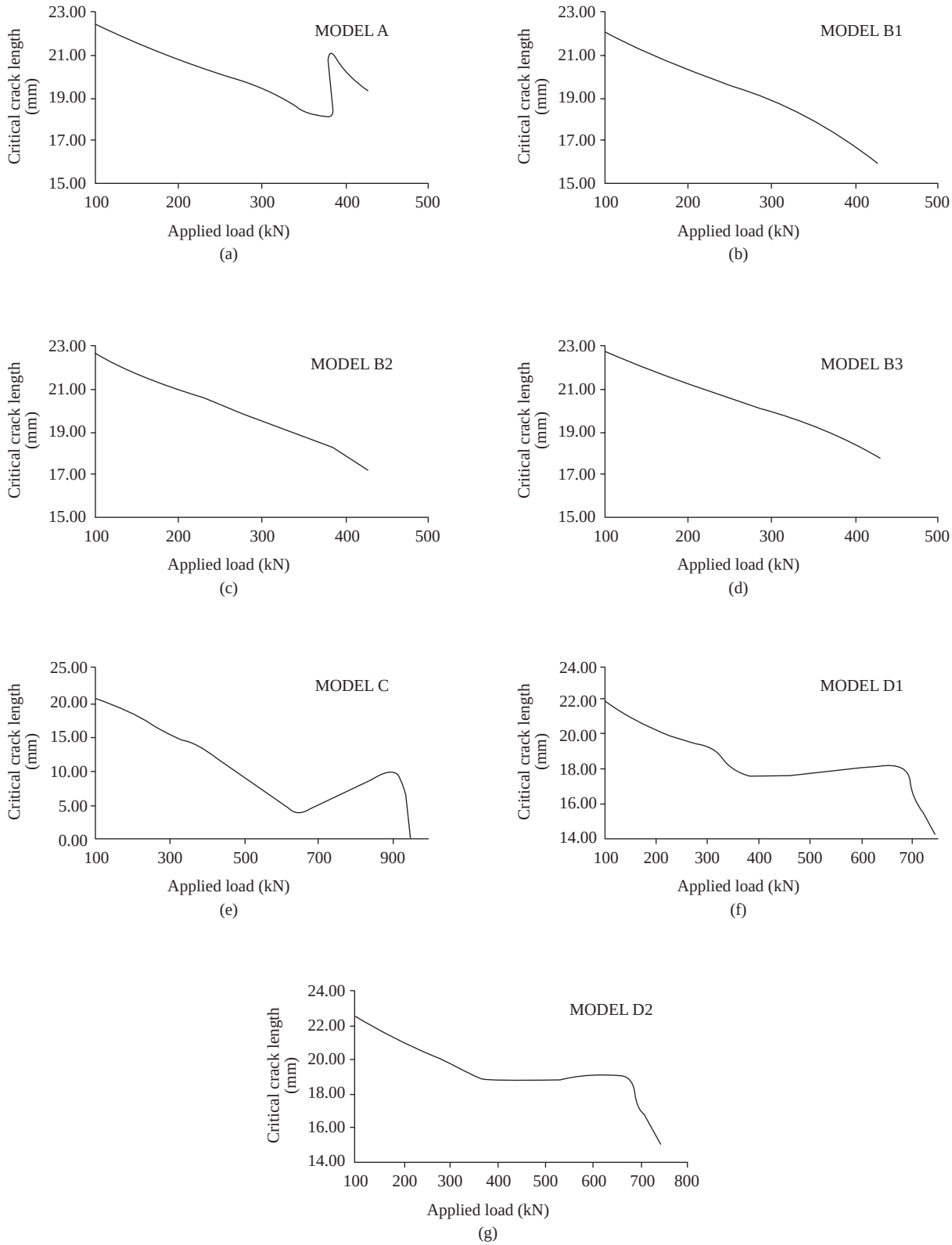

Figure 10. Variation of critical crack length versus applied load. a) Model A, b) Model B1, c) Model B2, d) Model B3, e) Model C, f) Model D1, g) Model D2.

Conclusions

The conclusions drawn can be summarized as follows:

- SINTAP provides an accurate evaluation of the fracture behavior of connections by considering the interaction of local fracture demands, crack size, connection geometry details and material properties.
- Use of cover plates, diaphragms and an additional haunch in beam-to-column connections increases the limit and maximum loads of welded structures.
- Limit and maximum loads that the structure can withstand unless collapse occurs are dependent on the yield and ultimate strengths. The fracture toughness of the weld material does not affect the limit or maximum load values.
- When strengthened connection types such as Models C and D are used in structures, there are 2 extreme critical crack lengths. The critical crack length decreases as the applied load reaches the limit load. When ligament collapse occurs, the critical crack length may be larger than that in the elastic region. That is, after yielding, relatively larger crack lengths can be permitted in the structure.
- Although it is expected that larger critical crack sizes can be permitted in strengthened connections with respect to weak connections such as Models A and B, the critical crack lengths of all connections become rather close to each other when the beam-to-column connections are subjected to loads at relatively low levels. The stress concentration due to the geometrical discontinuities in the strengthened connections causes this situation.
- Strengthened connections are safe when the structure is liable to instantaneous intense loads because they have relatively higher limit loads.

It can be concluded that reinforced connections are the most suitable for structures in seismic areas. The use of cover plates, a haunch section and a diaphragm increases the performance of the connections.

Acknowledgments

The authors wish to thank Dr. Mustafa Koçak and Dr. Afshin Motarjemi (GKSS Research Center, Germany) for their valuable guidance and help.

Nomenclature

a	crack length
a_i^W	distance from the centroid of the welded region to the neutral axis
a_i^B	distance from the centroid of the base metal region to the neutral axis
c	crack width
F	applied load
F_y	limit (yield) load
$f(L_r)$	failure assessment curve function
I	moment of inertia for area
L_r	F/F_y
K_I	stress intensity factor
K_r	K_I/K_{mat}
K_{mat}	material fracture toughness
M_y	limit (yield) moment
t_{bb}	cover plate thickness
t_{bf}	beam flange thickness
σ	remotely applied stress
σ_y^B	yield strength for base metal
σ_y^W	yield strength for weld metal

References

Ainsworth, R.A., Bannister, A.C. and Zerbst U. "An Overview of the European Flaw Assessment Procedure SINTAP and Its Validation", International Journal of Pressure Vessels and Piping, 77, 869-876, 2002.

American Welding Society, "Background for Eurocode 3- Part 2- Annex 3.1", Florida, 2000.

Azuma, K., Kurobane, Y. and Makino, Y., Cyclic Testing of Beam-to-Column Connections with Weld Defects and Assessment of Safety of Numerically Modeled Connections from Brittle Fracture", Engng. Structures, 22, 1596-1608, 2000.

Chi, W.M., "Prediction of Steel Connection Failure Using Computational Fracture Mechanics", PhD Thesis, Stanford University, 1999.

Fisher, J., Dexter, R.J. and Kaufmann, E.J., "Fracture Mechanics of Welded Structural Steel Connections", American Welding Society (AWS), 1997.

Kim, Y-J., Koçak, M., Ainsworth, R.A. and Zerbst, U., "SINTAP Defect Assessment Procedure for Strength Mis-Match Structures", Engineering Fracture Mechanics, 67, 529-546, 2000.

Kim, Y-J. and Schwalbe, K.H., "Mis-Match Effect on Plastic Yield Loads in Idealised Weldments II. Heat Affected Zone Cracks", Engineering Fracture Mechanics, 68, 529-546, 2001.

Kim, Y.J., Shim, D. and Nikbin, K., "Finite Element Based Plastic Limit Loads for Cylinders with Part-through Surface Cracks under Combined Loading", International Journal of Pressure Vessels and Piping, 80, 527-540, 2003.

Koçak, M. and Motarjemi, A.K., "Structural Integrity of Advanced Welded Structures". In: IIW Int. Conf., on Advanced Processes and Technologies in Welding and Allied Processes, Copenhagen, Denmark, 2002.

Kuntiyawichai, K. and Burdekin, F.M., "Engineering Assessment of Cracked Structures Subjected to Dynamic Loads Using Fracture Mechanics Assessment", Engineering Fracture Mechanics, 70, 1991-2014, 2003.

Motarjemi, A.K. and Koçak, M., "Fracture Assessment of a Clad Steel Using Various SINTAP Defect Assessment Procedure Levels", Fatigue Fracture Engineering Material & Structure, 25, 929-939, 2002.

Murakami, Y., Stress Intensity Factors Handbook, Pergamon Press, Oxford, 1987.

Rahman, S., "Net-Section-Collapse Analysis of Circumferentially Cracked Cylinders-Part I: Idealized Cracks and Closed-Form Solutions", Engineering Fracture Mechanics, 61, 191-211, 1998.

Rahman, S., "Net-Section-Collapse Analysis of Circumferentially Cracked Cylinders-Part II: Arbitrary-Shaped Cracks and Generalized Equations", Engineering Fracture Mechanics, 61, 213-230, 1998.

Righiniotis, T.D., Omer, E. and Elghazouli, A.Y., "A Simplified Crack Model for Weld Fracture in Steel Moment Connections", Engineering Structures, 24, 1133-1140, 2002.

Toyoda, M., "Properties of Steel Structures Damaged in Hanshin-Japan and Northridge-USA Earthquakes", Seminar Notes, Dokuz Eylül University, İzmir, Turkey, 15 March, 2002.